Lipidomics in Ulcerative Colitis Reveal Alteration in Mucosal Lipid Composition Associated with the Disease State

Joseph Diab, MSc,[a] Terkel Hansen, PhD,[a] Rasmus Goll, PhD, MD,[b, c] Hans Stenlund, PhD,[d]

Maria Ahnlund, PhD,[d] Einar Jensen, PhD ,[a] Thomas Moritz, PhD,[c]

Jon Florholmen, PhD, MD,[b, c] and Guro Forsdahl, PhD, [a]

[a] Natural Products and Medicinal Chemistry Research Group, Department of Pharmacy

Faculty of Health Sciences, University of Tromsø The Arctic University of Norway, Tromsø, Norway

[b] Research Group of Gastroenterology and Nutrition, Department of Clinical Medicine

Faculty of Health Sciences, University of Tromsø The Arctic University of Norway, Tromsø, Norway

[c] Department of Medical Gastroenterology, University Hospital of North Norway, Tromsø, Norway

[d] Swedish Metabolomics Center, Department of Molecular Biology, Umeå University, Umeå, Sweden

Corresponding author: Guro Forsdahl.

Department of pharmacy, University of Tromsø The Arctic University of Norway

Muninbakken 11, 9019, Tromsø, Norway

Guro.forsdahl@uit.no

+4791561129

This project was funded by the Northern Norway Regional Health Authority [SFP-1134-13], and university of Tromsø the arctic university of Norway.

Summary: The lipidomics analysis of mucosal lipids in UC patients revealed disruption in lipid composition pattern in active and deep remission UC. Several lipids seem to be involved in the inflammatory processes in UC, and could reflect the disease state.

Abstract

Background

The onset of ulcerative colitis (UC) is associated with alterations in lipid metabolism, and a disruption of the balance between pro and anti-inflammatory molecules. Only a few studies describe the mucosal lipid bio-signatures during active UC. Moreover, the dynamics of lipid metabolism in the remission state is poorly defined. Therefore, this study aims to characterize mucosal lipid profiles in treatment-naive UC patients, and deep remission UC patients, compared to healthy subjects.

Methods

Treatment-naive UC patients (n=21), UC patients in deep remission (n=12), and healthy volunteers (n=14) were recruited. The state of deep remission was defined by histological and immunological remission defined by a normalized TNF-α gene expression. Mucosa biopsies were collected by colonoscopy. Lipid analysis was performed by means of ultra-high performance liquid chromatography coupled with tandem mass spectrometry (UPLC-MS-MS). In total, 220 lipids from 11 lipid classes were identified.

Results

The relative concentration of 122 and 36 lipids was altered in UC treatment-naïve patients and UC remission patients, respectively, compared with healthy controls. The highest number of significant variations were in phosphatidylcholines (PC), ceramides (Cer), and sphingomyelin (SM) composition. Multivariate analysis revealed discrimination among the study groups based on the lipid profile. Furthermore, changes in PE(38:3), Cer(d18:1/24:0), and Cer(d18:1/24:2), were most distinctive between the groups.

Conclusion

This study revealed alteration in mucosal lipid composition pattern in treatment-naïve UC and deep remission UC. We report several distinctive lipids, which might be involved in the inflammatory response in UC, and could reflect the disease state.

Key Words

Inflammatory bowel disease; Lipidomics; Ulcerative colitis; Phospholipids; Sphingolipids.

1- Introduction

Inflammatory bowel diseases (IBD) are chronic, relapsing inflammatory disorders in the gastrointestinal tract that affects around 1.6 million in the United States and 2.2 million in Europe[1]. The two major forms of IBD, ulcerative colitis (UC) and Crohn's disease (CD), are characterized by a dysregulated mucosal immune response triggered by the intestinal commensal flora[2]. Several genetic, bacterial, and environmental factors appear to lead to the onset of IBD. However, the etiology of IBD is not fully understood[3]. The main treatments of IBD involve steroids and immune-suppressive/modulatory medications[4], such as anti-TNF-α in severe cases. However, 20-30% of UC patients need surgery at some point during their lifetime due to treatment failure or disease complications[5], whereas 50-65% of UC patients might achieve remission[6]. Nonetheless, since there is no agreement on the definition of 'complete remission' state, IBD patients might relapse after de-escalating medical treatment[7].

Membrane bio-active lipids modulate the immune response by functioning as intra- and intercellular signaling molecules[8]. For instance, sphingolipids and phospholipids are involved in controlling cellular processes, such as proliferation, migration, apoptosis, differentiation, and pro-inflammatory cytokine release[9, 10]. Accordingly, the chronic inflammation seen in IBD is characterized by a disruption of the balance between pro- and anti-inflammatory molecules[11]. Consequently, UC seems to be associated with alterations in the lipid metabolism[12, 13]. Furthermore, we have recently demonstrated major changes in the mucosal concentration of poly-unsaturated fatty acid (PUFA) metabolites in treatment naive UC patients[14].

'Lipidomics' is defined as the study of the lipids metabolism, composition, and distribution on a large scale in a given organism[15]. Lipidomics has become a powerful tool to understand the pathology and to predict the prognosis of complex inflammatory diseases such as, diabetes mellitus[16, 17], multiple sclerosis[18], arthritis[19], and Alzheimer disease[20]. However, there are few IBD studies describing mucosal lipid bio-signatures.

This study aims to describe the mucosal lipid profile in treatment naive UC patients and deep remission UC patients compared with healthy subjects. The high throughput lipidomics analysis will help capturing the main mucosal lipid composition changes, which reflect the inflammatory state in active UC and treatment-induced deep remission UC.

2- Materials and Methods

2-1-Patients and biopsy collection

Mucosal biopsies were collected from newly diagnosed treatment naive UC patients (n=21) and UC patients in deep remission (n=12). The UC diagnosis was established upon clinical, endoscopic and histological criteria defined by the European Crohn and Colitis Organization (ECCO) guidelines.[21] The degree of inflammation was evaluated during colonoscopy using the scoring system of ulcerative colitis disease activity index (UCDAI); UCDAI score of 3-5 is defined as mild, 6-8 as moderate, and 9-12 as severe UC[22]. TNF-α mRNA expression levels were measured by real-time PCR in mucosal biopsies, to evaluate the UC activity[23]. The state of deep remission was defined as endoscopic healed mucosa by ECCO 2017 consensus (Mayo score = 0)[24] and, additionally, normalized mucosal TNF-α level induced by anti-TNF- α treatment[25]. Subjects performing endoscopy for colonic malignancy screening, with normal findings and normal colonic histological examination, served as healthy controls (n=14).

The biopsies from UC treatment naive patients and the UC remission group were obtained from the rectum or sigmoid colon. In patients with active UC, biopsies were taken from the most inflamed mucosa, whereas biopsies from the control group were obtained from the rectum. The dry weight of the biopsies ranged from 2-8 mg. All biopsies were dry-frozen immediately at -70°C, and kept at this temperature until further analysis.

2-2-Chemicals and reagents

N-palmitoyl-d_{31}-D-erythro-sphingosine (16:0-d31 ceramide) was obtained from Avanti Polar Lipids (Alabaster, AL, USA). Tripalmitin-1,1,1-$^{13}C_3$ (TG(16:0/16:0/16:0)-$^{13}C_3$) was purchased from Larodan (Solna, Sweden). Acetonitrile, formic acid, ammonium formate, chloroform and methanol were HPLC grade or higher and purchased from Merck (Darmstadt, Germany). Isopropanol was obtained from VWR International (Stockholm, Sweden). Water was purified by a Milli-Q gradient system (Millipore, Milford, MA, USA).

2-3-Lipid Extraction

Lipid extraction was carried out using a modified Folch extraction[26]. Briefly, each biopsy was transferred to an Eppendorf tube and kept on ice. Then, the extraction mixture (chloroform:methanol 2:1 v/v, including both internal standards tripalmitin-1,1,1-$^{13}C_3$ and 16:0-d31 ceramide) was added to

the biopsy in a solid-to-solvent ratio of 1:50 (w/v). The final concentration of tripalmitin-1,1,1-$^{13}C_3$ and 16:0-d31 ceramide was 0.5 ng/mL and 2 ng/mL respectively. Two tungsten beads were added to each tube, and the samples shaken at 30 Hz for 3 min, and stored at room temperature for 30–60 min. The beads were removed, and the samples were further centrifuged at 14,000 rpm and 4 °C for 3 min. Finally, the organic phase was collected, split in half and transferred to two micro vials. Samples were dried using a vacuum concentrator (MIVac, SP, Warminster, PA, USA) reconstituted in 50 µL of acetonitrile. Extracts were stored at −80 °C until analysis.

2-4-Lipidomics analysis

Lipidomics analysis was performed with an Infinity 1290 Agilent (Agilent Technologies, Santa Clara, CA, USA) ultra-high performance liquid chromatograph coupled with tandem mass spectrometry (UHPLC-MS-MS) as previously described[26, 27]. Briefly, 1 µL of each extract was injected into the UHPLC system equipped with an Acquity column (CSH, 2.1× 50 mm, 1.7 µm C18 in combination with a 2.1 mm × 5 mm, 1.7 µm VanGuard CSH precolumn (Waters Corporation, Milford, MA, USA), held at 60 °C. The gradient elution buffers were A (60:40 acetonitrile: water, 10 mM ammonium formate containing 0.1% formic acid) and B (90:10 2-propanol: acetonitrile, 10 mM ammonium formate containing 0.1% formic acid). 15 % B at a flow rate of 0.5 mL/min was set as initial condition, and the following gradient was used: B was increased to 30 % in 1.2 min, then to 55% in 0.3 min and held at 55 % for 3.5 min. It was progressively increased as follows: 72% in 2 min, then 85% in 2.5 min and to 100% in 0.5 min and was held for 2 minutes. The exact masses of individual lipid molecules were detected with an Agilent 6550 Q- TOF mass spectrometer equipped with an iFunnel jet stream electrospray ion source (Agilent Technologies, Santa Clara, CA, USA). The first batch of extracts was analyzed in positive mode. Then, the instrument was switched to the negative mode and the second batch of extracts was injected. The flow gas temperature was set at 150°C, the drying gas flow at 12 L min^{-1} and the nebulizer pressure at 40 psi. The sheath gas temperature was set at 350°C and the sheath gas flow 1 L min^{-1}. The capillary voltage was set at 4000 V for the positive mode and 2300 V for the negative mode. The m/z range was 70 - 1700, and data were collected in centroid mode with an acquisition rate of 4 scans/s.

Targeted data processing was performed using Agilent MassHunter ProFinder B.08.00 software, whereas in- house databases with exact masses and experimental retention times were used for identification. Finally, the extracted features were aligned and matched between samples. In total, 220 lipid species were identified. These lipid species were from the following lipid classes and subclasses: dihydroceramide (dhCer), galactosylceramide (GalCer), ceramide (Cer), sphingomyelin (SM), phosphatidylethanolamine (PE), phosphatidylcholine (PC), phosphatidylserine (PS), phosphatidylinositol (PI), phosphatidylglycerol (PG) lysophosphatidylethanolamine (LPE), and lysophosphatidylcholine (LPC). Results were expressed as area under the curve (AUC) values from the extracted ion chromatograms of each lipid molecule. Peak areas of individual lipid species were normalized by the sum of peak areas of all detected lipid species in the same lipid class. Hence, quantitative data for each lipid specie was expressed in percentage as relative concentration to the total amount of lipids in the same respective lipid class.

2-5-Statistical analysis

Statistical analysis was carried out using MetaboAnalyst 4.0, a web tool for metabolomics data analysis (http://www.metaboanalyst.ca/)[28] . Undetectable lipids, which represented 1.2% of total reported lipids, were assigned a value corresponding to half of the minimum positive value in the original data. Shapiro–Wilk test of normality was applied, and the data was not found normally distributed. Kruskal–Wallis one way analysis of variance test was performed to determine the differences of lipid species between treatment naïve UC, remission UC, and control groups. Acquired *p*-values were adjusted using Benjamini and Hochberg FDR method[29]. Dunn's test[30] was applied as a post hoc test, and significant *p*-value cut-off was corrected to 0.017 by Bonferroni multiple comparison method[31]. The relative lipid concentrations were auto scaled in order to adjust the importance of high and low abundance lipids to an equal level, and to ease the comparison between the relative lipid concentrations among the study groups[32]. Multivariate analysis was carried out using SIMCA software (version 14.0.0.135559; Umetrics AB, Umea, Sweden). Unsupervised multivariate analysis principle component analysis (PCA) was first performed to assess the unicity of the lipidome for each of the study group. Then, supervised orthogonal partial least squares projection to latent structures-discriminant analysis (OPLS-DA) was employed and shared and unique plots (SUS-plot)[33] were generated to identify the main lipids responsible for the

discriminant lipid profile associated with UC treatment-naïve patients. The parameters of the OPLS-DA model were described by R^2X_{cum}, R^2Y_{cum} and Q^2_{cum}, whereas, R^2X_{cum} is the cumulative modeled variation in X, R^2Y_{cum} is the amount of variation in X correlated to Y (response matrix) and Q^2_{cum} is the cumulative predicted ability of the model[34].

3- Ethical Considerations

The Regional Committee of Medical Ethics of North Norway and the Norwegian Social Science Data Services approved the study and the storage of biological material under the number (REK NORD 2012/1349). In addition, all enrolled subjects have signed an informed consent form.

4- Results

4-1-Subjects Characteristics

In total, 21 newly diagnosed treatment naive UC patients, 12 UC patients in state of deep remission and 14 healthy controls were enrolled in this study. The study group characteristics are described in Table 1. The UC patients' disease activity was ranging from mild to severe; 11 patients had mild UC, 4 patients had moderate UC and 6 patients had severe UC.

4-2-Mucosal lipid profiles in treatment-naive UC patients, UC remission patients and controls

Mucosal lipid profiles in colon biopsies were assessed to determine significant changes in lipid composition in treatment naive patients and UC deep remission patients compared to controls.

Kruskall-Wallis one way analysis of variance with Dunn post hoc was used to compare lipid concentrations between all three groups (supplementary Table 1). As summarized in Table 2, among the 220 lipids included in this study, the relative concentration of 122 and 67 lipids were altered in UC treatment naïve patients compared with healthy controls and with UC remission patients respectively. However, the mucosal relative concentration of only 26 lipids was changed in UC remission patients compared with healthy controls. The lipid classes with the highest number of significant variation in the lipid composition were PC, Cer, and SM.

The greatest change was in the relative mucosal concentration of PE(38:3), which was increased by 37 fold in inflamed mucosa compared with healthy mucosa (supplementary Table 1).

4-3-Discriminative models for UC state

The PCA was used as an unbiased multivariate analysis to assess the distinctive lipidomic profile for each of the study groups. The PCA score plot (Figure 1A) revealed a clear separation between naïve treatment UC patients and healthy controls indicating a specific lipidomic profile for active UC patients. However, PCA did not reveal a distinct lipidomic profile for UC remission patients. In addition, PCA provided no separation of patients according to age, sex or activity score (data not shown). A supervised OPLS-DA was applied to assess the discriminative power of the mucosal lipid profile for UC patients (in active and remission state) and healthy controls. A significant OPLS-DA model was obtained with maximum separation between the study groups (Figure 1B). The performance parameters describing the fitness of all multivariate data analysis models in this study are described in table 3.

4-4-Discriminative lipids for UC state

Two OPLS DA models were built, UC treatment-naive vs healthy controls and UC treatment-naive vs UC remission. The score plots corresponding to these models are shown in Figures 1C and 1D respectively. The shared and unique structure (SUS) plot, constructed from the loading plots of these models, identified the main lipid composition pattern in treatment naïve UC patients (Figure 2A). The SUS plot revealed that the lipidomic profile in UC treatment-naïve patients is mainly characterized by high levels of very long fatty acid chain (VLCFA) ceramides, specifically those with 24 carbons chain-length (C24). In addition, several PCs and PEs were elevated, mainly PE(38:3).

Based on the SUS-plot, 3 candidate lipids were selected for further investigation. These lipids were PE(38:3), Cer(d18:1/24:0), and Cer(d18:1/24:2). The discriminative ability of these lipids was confirmed by comparing the ion chromatograms at the specific retention times (RT) for each of these lipids among the study groups. As shown in Figure 2, PE(38:3) was only detected in UC patients colonic mucosa (both UC active and UC remission patients). Moreover, PE(38:3) is clearly increased in inflamed mucosa (UC active) compared with healed mucosa (UC remission). In addition, the levels of Cer(d18:1/24:0) and Cer(d18:1/24:2) were low in healed mucosa, and increased in a step wise manner in UC remission patients and treatment-naïve UC patients.

5-Discussion

This study provides a unique and detailed characterization of mucosal lipid profiles in treatment naive newly diagnosed and deep remission UC patients. Previous studies were restricted to investigate lipid profiles in other matrices, specifically plasma[35] and stool[36] or in animal models with experimentally induced colitis [37]. Moreover, previous studies were performed on a mix of treated and untreated UC patients, which might lead to less specific profiles, regarding the differences between active disease and remission demonstrated in the present data. Therefore, only treatment naive UC patients were recruited as active inflammation group in our study. The state of remission was based on a combination of normalized TNF gene expression, histologic, and endoscopic criteria (Mayo = 0). This allows the detection of variations in the lipid composition that are exclusively associated with UC development. To our knowledge, this is the first published study of mucosal lipid profiles in UC patients. We have investigated 220 lipids from 11 different lipid classes. The lipid profiling revealed major disruption in the mucosal lipid composition in active UC patients compared with healthy controls.

The most significant finding in the current study is the observed changes in the PE(38:3) concentration in response to the mucosal inflammatory state. This lipid was only detected in the UC patients' mucosa. Notably, the mucosal levels consistently decrease in the remission state compared with the active disease state. Despite being poorly described in UC, high level of serum PE(38:3) was previously found associated with diabetes and prediabetes[38]. Moreover, increased level of PE has been linked with Alzheimer disease[39]. In addition, due to the role of PE in apoptosis, PE has been suggested as a target for cell death imaging, and a marker for TNF-induced inflammation[40, 41]. The plausible role of PE(38:3) in promoting inflammation could make it useful in monitoring the development of UC. However, this needs to be confirmed by larger studies, which also investigate the presence of PE(38:3) in other kinds of matrices such as feces, serum, or urine.

In the present data, Cer(d18:1/24:2) and Cer(d18:1/24:0) increase according to the UC state from remission to active inflammation. These two ceramides, classified as very long chain fatty acid sphingolipids (VLCFAs), are necessary for the neutrophils functions[42]. The present research is the first report highlighting the importance of VLCFA ceramides in UC, although they have been reported

involved in other inflammatory diseases. For instance, higher levels of Cer(d18:1/24:2) and Cer(d18:1/24:0) were detected in synovial fluid in rheumatoid arthritis and osteoarthritis patients[43]. Moreover, a high serum level of Cer(d18:1/24:0) has been associated with a high risk of dementia in Alzheimer disease, and increased with the disease severity[44].

The highest significant variations in the lipid composition were detected in Cer, SM and PC profiles. Previously, lipids analysis on experimentally induced IBD have revealed changes in sphingolipids (Cer and SM)[45] and the PC profile[46]. Changes in the PC profile demonstrate the impairment in the mucus barrier during IBD[47]. Furthermore, changes in sphingolipids could be explained by the suggested harmful role of ceramides in IBD, mainly by activating immune cells and triggering apoptosis[9]. Consequently, tissue ceramide levels were found elevated in a stepwise manner from control to remission, mild, and moderate/severe IBD patients[48]. In addition, it has been previously found that IL-1 stimulates ceramide accumulation in intestinal epithelial cells[49]. Moreover, previous studies revealed major changes in sphingolipid metabolic pathways during IBD[50, 51]. The current study has revealed a distinct lipid profile in UC deep remission patients, although being selected based on mucosal healing and immunological remission[52]. Accordingly, the mucosal concentrations of 26 lipid species, mainly sphingolipids, were altered compared to healthy control. This finding could be of clinical utility in defining treatment goals and end-point parameters in the context of personalized medicine. Furthermore, it supports previously published data on the sphingolipid metabolism as a therapeutic target in IBD[53, 54]. Moreover, this suggests the lipidomics profiling as a tool to improve the definition of UC remission in the current guidelines and scoring systems.

The present work is purely descriptive. Moreover, the relatively small sample size in the current study disqualify subgroup analysis according to the severity of the diseases. Furthermore, the reported results are expletory and need to be validated by a larger cohort. In addition, we suggest exploring the mucosal lipid profile using targeted analytical approaches allowing the absolute quantification of the studied lipids.

6-Conclusion

The present report describe an in depth the mucosal lipid profile in UC via full lipidomic analysis of colon biopsies taken from UC treatment naive patients, UC patients in state of deep remission, and healthy subjects. The analysis of mucosal lipids demonstrated alteration in the lipid composition in active and deep remission UC, and it revealed the involvement of several lipids in the mucosal inflammatory processes in UC.

Acknowledgments

We thank Renate Meyer for administrating the patient samples. The Northern Norway Regional Health Authority [SFP-1134-13], and university of Tromsø the arctic university of Norway funded this project.

Reference

1. M'Koma AE. Diagnosis of inflammatory bowel disease: Potential role of molecular biometrics. World J Gastrointest Surg 2014;6:208-19.
2. Molodecky NA, Kaplan GG. Environmental Risk Factors for Inflammatory Bowel Disease. Gastroenterol Hepatol (N Y) 2010;6:339-346.
3. Ananthakrishnan AN, Bernstein CN, Iliopoulos D, et al. Environmental triggers in IBD: a review of progress and evidence. Nature Reviews Gastroenterology &Amp; Hepatology 2017;15:39.
4. Bernstein CN. Treatment of IBD: Where We Are and Where We Are Going. The American Journal Of Gastroenterology 2014;110:114.
5. Ferrari L, Krane MK, Fichera A. Inflammatory bowel disease surgery in the biologic era. World Journal of Gastrointestinal Surgery 2016;8:363-370.
6. Actis GC, Pellicano R. Inflammatory bowel disease: Efficient remission maintenance is crucial for cost containment. World journal of gastrointestinal pharmacology and therapeutics 2017;8:114-119.
7. Bryant RV, Winer S, Spl T, et al. Systematic review: Histological remission in inflammatory bowel disease. Is ‘complete’ remission the new treatment paradigm? An IOIBD initiative. Journal of Crohn's and Colitis 2014;8:1582-1597.
8. Shores DR, Binion DG, Freeman BA, et al. New Insights into the Role of Fatty Acids in the Pathogenesis and Resolution of Inflammatory Bowel Disease. Inflammatory bowel diseases 2011;17:2192-2204.
9. Bryan P-F, Karla C, Edgar Alejandro M-T, et al. Sphingolipids as Mediators in the Crosstalk between Microbiota and Intestinal Cells: Implications for Inflammatory Bowel Disease. Mediators of Inflammation 2016;2016:9890141.

10. Sewell GW, Hannun YA, Han X, et al. Lipidomic profiling in Crohn's disease: Abnormalities in phosphatidylinositols, with preservation of ceramide, phosphatidylcholine and phosphatidylserine composition. The International Journal of Biochemistry & Cell Biology 2012;44:1839-1846.

11. Das UN. Inflammatory bowel disease as a disorder of an imbalance between pro- and anti-inflammatory molecules and deficiency of resolution bioactive lipids. Lipids Health Dis 2016;15:11-18.

12. Masoodi M, Pearl DS, Eiden M, et al. Altered colonic mucosal Polyunsaturated Fatty Acid (PUFA) derived lipid mediators in ulcerative colitis: new insight into relationship with disease activity and pathophysiology. PLoS One 2013;8:e76532.

13. Schniers A, Goll R, Pasing Y, et al. Ulcerative colitis: functional analysis of the in-depth proteome. Clinical Proteomics 2019;16:4.

14. Diab J, Al-Mahdi R, Gouveia-Figueira S, et al. A Quantitative Analysis of Colonic Mucosal Oxylipins and Endocannabinoids in Treatment-Naïve and Deep Remission Ulcerative Colitis Patients and the Potential Link With Cytokine Gene Expression. Inflammatory Bowel Diseases 2018:izy349-izy349.

15. Lydic TA, Goo YH. Lipidomics unveils the complexity of the lipidome in metabolic diseases. Clin Transl Med 2018;7:4.

16. Suvitaival T, Bondia-Pons I, Yetukuri L, et al. Lipidome as a predictive tool in progression to type 2 diabetes in Finnish men. Metabolism 2018;78:1-12.

17. Pinz I, Robich MP, Ryzhov S, et al. A Novel Lipidomic Approach to Understand Human Diabetic Heart Disease. The FASEB Journal 2017;31:883.19-883.19.

18. Bergholt MS, Serio A, McKenzie JS, et al. Correlated Heterospectral Lipidomics for Biomolecular Profiling of Remyelination in Multiple Sclerosis. ACS Cent Sci 2018;4:39-51.

19. Surowiec I, Ärlestig L, Rantapää-Dahlqvist S, et al. Metabolite and Lipid Profiling of Biobank Plasma Samples Collected Prior to Onset of Rheumatoid Arthritis. PLOS ONE 2016;11:e0164196.

20. Naudi A, Cabre R, Jove M, et al. Lipidomics of human brain aging and Alzheimer's disease pathology. Int Rev Neurobiol 2015;122:133-89.

21. Stange EF, Travis SP, Vermeire S, et al. European evidence-based Consensus on the diagnosis and management of ulcerative colitis: Definitions and diagnosis. J Crohns Colitis 2008;2:1-23.

22. Marteau P, Probert CS, Lindgren S, et al. Combined oral and enema treatment with Pentasa (mesalazine) is superior to oral therapy alone in patients with extensive mild/moderate active ulcerative colitis: a randomised, double blind, placebo controlled study. Gut 2005;54:960-5.

23. Olsen T, Goll R, Cui G, et al. Tissue levels of tumor necrosis factor-alpha correlates with grade of inflammation in untreated ulcerative colitis. Scand J Gastroenterol 2007;42:1312-1320.

24. Magro F, Gionchetti P, Eliakim R, et al. Third European Evidence-based Consensus on Diagnosis and Management of Ulcerative Colitis. Part 1: Definitions, Diagnosis, Extra-intestinal Manifestations, Pregnancy, Cancer Surveillance, Surgery, and Ileo-anal Pouch Disorders. J Crohns Colitis 2017;11:649-670.

25. Johnsen KM, Goll R, Hansen V, et al. Repeated intensified infliximab induction - results from an 11-year prospective study of ulcerative colitis using a novel treatment algorithm. Eur J Gastroenterol Hepatol 2017;29:98-104.

26. Nygren H, Seppanen-Laakso T, Castillo S, et al. Liquid chromatography-mass spectrometry (LC-MS)-based lipidomics for studies of body fluids and tissues. Methods Mol Biol 2011;708:247-57.

27. Orikiiriza J, Surowiec I, Lindquist E, et al. Lipid response patterns in acute phase paediatric Plasmodium falciparum malaria. Metabolomics 2017;13:41.

28. Chong J, Soufan O, Li C, et al. MetaboAnalyst 4.0: towards more transparent and integrative metabolomics analysis. Nucleic Acids Research 2018;46:W486-W494.

29. Benjamini Y, Hochberg Y. Controlling the False Discovery Rate: A Practical and Powerful Approach to Multiple Testing. Journal of the Royal Statistical Society. Series B (Methodological) 1995;57:289-300.

30. Dunn OJ. Multiple Comparisons among Means. Journal of the American Statistical Association 1961;56:52-64.

31. Bonferroni CE. Teoria statistica delle classi e calcolo delle probabilit\`{a}. Pubblicazioni del R Istituto Superiore di Scienze Economiche e Commerciali di Firenze 1936;8:3-62.

32. van den Berg RA, Hoefsloot HC, Westerhuis JA, et al. Centering, scaling, and transformations: improving the biological information content of metabolomics data. BMC Genomics 2006;7:142.

33. Wiklund S, Johansson E, Sjostrom L, et al. Visualization of GC/TOF-MS-based metabolomics data for identification of biochemically interesting compounds using OPLS class models. Anal Chem 2008;80:115-22.

34. Ni Y, Su M, Lin J, et al. Metabolic profiling reveals disorder of amino acid metabolism in four brain regions from a rat model of chronic unpredictable mild stress. FEBS Lett 2008;582:2627-36.

35. Fan F, Mundra PA, Fang L, et al. Lipidomic Profiling in Inflammatory Bowel Disease: Comparison Between Ulcerative Colitis and Crohn's Disease. Inflamm Bowel Dis 2015;21:1511-8.

36. Davies JM, Hua H-U, Dheer R, et al. Stool Phospholipid Signature is Altered by Diet and Tumors. PLOS ONE 2014;9:e114352.

37. Lee Y, Choo J, Kim SJ, et al. Analysis of endogenous lipids during intestinal wound healing. PLOS ONE 2017;12:e0183028.

38. Meikle PJ, Wong G, Barlow CK, et al. Plasma Lipid Profiling Shows Similar Associations with Prediabetes and Type 2 Diabetes. PLOS ONE 2013;8:e74341.

39. Calzada E, Onguka O, Claypool SM. Phosphatidylethanolamine Metabolism in Health and Disease. In: Jeon KW, ed. International Review of Cell and Molecular Biology. Volume 321: Academic Press, 2016:29-88.

40. Elvas F, Stroobants S, Wyffels L. Phosphatidylethanolamine targeting for cell death imaging in early treatment response evaluation and disease diagnosis. Apoptosis 2017;22:971-987.

41. Delvaeye T, Wyffels L, Deleye S, et al. Noninvasive Whole-Body Imaging of Phosphatidylethanolamine as a Cell Death Marker Using (99m)Tc-Duramycin During TNF-Induced SIRS. J Nucl Med 2018;59:1140-1145.

42. Sassa T, Kihara A. Metabolism of Very Long-Chain Fatty Acids: Genes and Pathophysiology. Biomolecules & Therapeutics 2014;22:83-92.

43. Kosinska MK, Liebisch G, Lochnit G, et al. Sphingolipids in human synovial fluid--a lipidomic study. PLoS One 2014;9:e91769.

44. Mielke MM, Bandaru VVR, Haughey NJ, et al. Serum ceramides increase the risk of Alzheimer disease: The Women's Health and Aging Study II. Neurology 2012;79:633-641.

45. Qi Y, Jiang C, Tanaka N, et al. PPARalpha-dependent exacerbation of experimental colitis by the hypolipidemic drug fenofibrate. Am J Physiol Gastrointest Liver Physiol 2014;307:G564-73.

46. Wang R, Gu X, Dai W, et al. A lipidomics investigation into the intervention of celastrol in experimental colitis. Mol Biosyst 2016;12:1436-44.

47. Ehehalt R, Wagenblast J, Erben G, et al. Phosphatidylcholine and lysophosphatidylcholine in intestinal mucus of ulcerative colitis patients. A quantitative approach by nanoelectrospray- tandem mass spectrometry. Scandinavian Journal of Gastroenterology 2004;39:737-742.

48. Suh JH, Degagne E, Gleghorn EE, et al. Sphingosine-1-Phosphate Signaling and Metabolism Gene Signature in Pediatric Inflammatory Bowel Disease: A Matched-case Control Pilot Study. Inflamm Bowel Dis 2018;24:1321-1334.

49. Homaidan F, E El-Sabban M, Chakroun I, et al. IL-1 stimulates ceramide accumulation without inducing apoptosis in intestinal epithelial cells, 2002.

50. Pulkoski-Gross MJ, Uys JD, Orr-Gandy KA, et al. Novel sphingosine kinase-1 inhibitor, LCL351, reduces immune responses in murine DSS-induced colitis. Prostaglandins & Other Lipid Mediators 2017;130:47-56.

51. Snider AJ, Wu BX, Jenkins RW, et al. Loss of neutral ceramidase increases inflammation in a mouse model of inflammatory bowel disease. Prostaglandins & Other Lipid Mediators 2012;99:124-130.

52. Florholmen J. Mucosal healing in the era of biologic agents in treatment of inflammatory bowel disease. Scand J Gastroenterol 2015;50:43-52.

53. Abdel Hadi L, Di Vito C, Riboni L. Fostering Inflammatory Bowel Disease: Sphingolipid Strategies to Join Forces. Mediators of Inflammation 2016;2016:13.

54. Raad MA, Chams NH, Sharara AI. New and Evolving Immunotherapy in Inflammatory Bowel Disease. Inflammatory intestinal diseases 2016;1:85-95.

Figures legends

Figure 1. Multivariate analysis of the mucosal lipid profiles. Each subject was labeled according to the corresponding study group. Figure 2.A: 2D Principle component analysis (PCA) score plots. The variation explained by PC1 and PC2 were 25.1% and 18.5%, respectively. Figure 2.B: The score plot of the OPLS-DA model built from the lipid profile of the three study groups. Figure 2.C and Figure 2.D: Score plot of the OPLS-DA model built from the lipid profile of UC treatment naïve vs healthy controls and UC treatment naïve vs UC remission patients.

Figure 2: Figure 2.A SUS-plot constructed using the correlation coefficient (p (corr)) from the loading plots of the two OPLS DA models, UC treatment-naïve vs Controls (X-axis) and UC treatment-naïve vs UC remission (Y-axis). The lipids are labelled according to lipid class. The highlighted region contains lipids that are elevated in UC treatment naïve patients. For simplicity, only a few lipids are displayed with full name. The same figure with all full names of the lipids is provided in the supplementary data section (supplementary Figure 1). Figures 3B, 3C and 3D represent the extracted ion chromatograms of PE(38:3), Cer(d18:1/24:0), and Cer(d18:1/24:2), respectively. The peaks are aligned and colored according to the study group. Black is the treatment-naïve UC group, red is UC deep remission group, and green is healthy control group.

Tables

Table 1. Description of study group characteristics.

Study Group	Number of Subjects	Age* year	Sex Female/Male	TNF-α* copies/μg of total RNA
Active UC (debut)	21	42 (20-68)	6/15	17670 (4600-30700)
Healthy controls	14	54 (26-83)	5/9	5400 (1800-13600)
UC remission	12	48 (23-71)	4/8	4675 (800-7300)

*****Data are presented as mean (range)

Table 2: Summary of altered lipids associated with UC state identified by Kruskall-Wallis and Dunn post-hoc analysis

	Number of lipids			
Lipid Class	Total number of annotated lipids	Active UC vs Healthy Control	Active UC vs UC Remission	UC Remission vs Healthy Control
Phosphatidylcholine	55	40	18	4
Ceramide	27	14	10	5
Phosphatidylserine	20	11	8	1
Phosphatidylinositol	14	9	5	1
Phosphatidylethanolamine	25	10	8	3
Galactosylceramide	20	13	5	3
Sphingomyelin	19	10	7	2
Dihydroceramide	17	7	5	7
Phosphatidylglycerol	6	1	1	-
Lysophasphatidylcholine	12	4	-	2
Lysophasphatidylethanolamine	5	3	-	-
Total	220	122	67	26

Table 3: Summary performance parameters of multivariate data analysis models applied in this study.

Data set	Model	Components	R^2X_{cum}	R^2Y_{cum}	Q^2_{cum}
All 3 study groups	PCA	2	0.436	-	0.302
All 3 study groups	OPLS-DA	2 + 1*	0.553	0.762	0.580
Active UC vs UC Remission	OPLS-DA	1+1*	0.403	0.868	0.788
UC Remission vs Healthy Control	OPLS-DA	1+1*	0.332	0.756	0.584

* The number of predictive components followed by the number of orthogonal components.

Figure 1

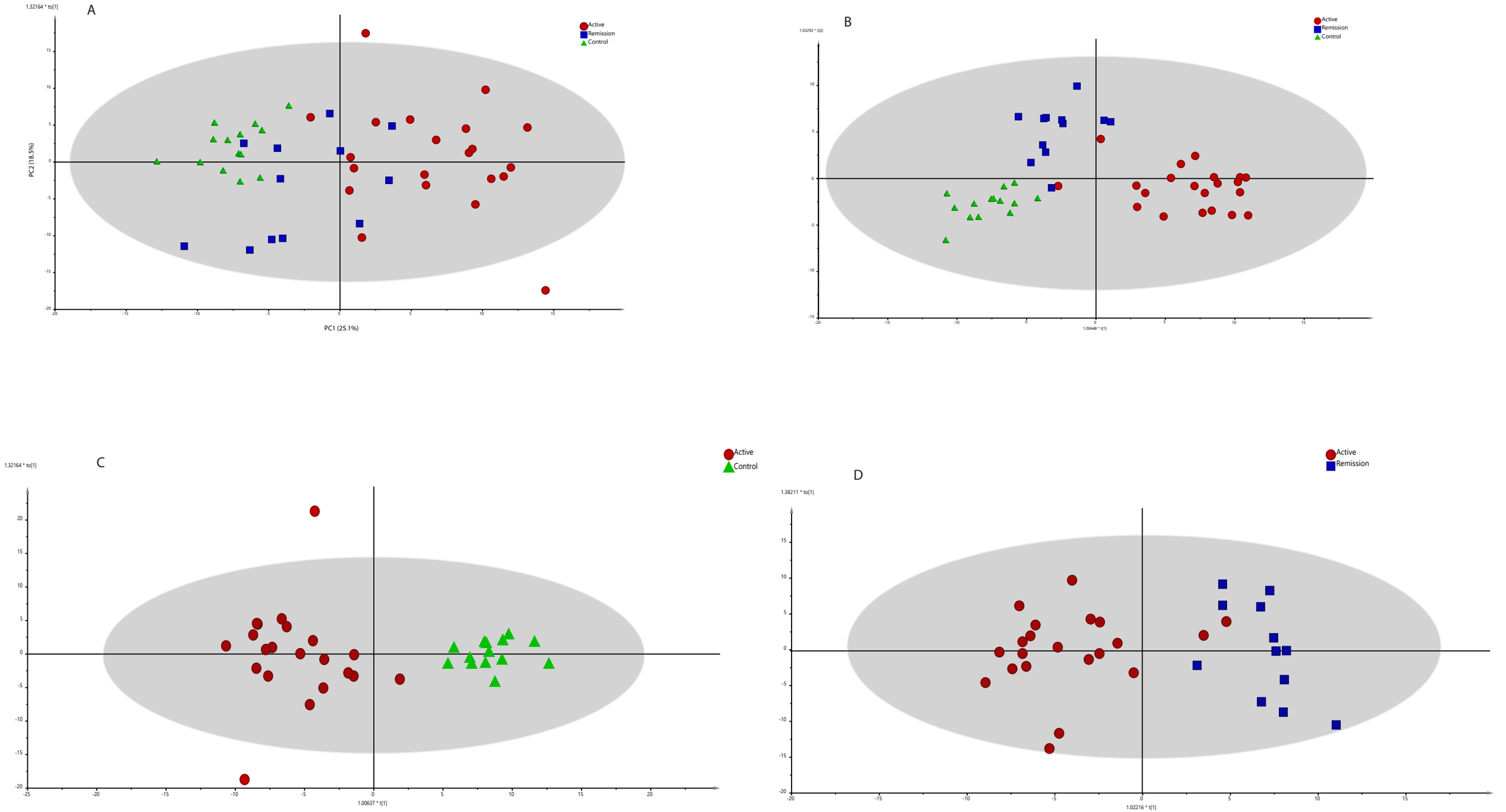
A
1.32164 * to[1]
PC2 (18.5%)
PC1 (25.1%)
Active
Remission
Control
B
1.03292 * t[2]
1.00448 * t[1]
Active
Remission
Control
C
1.32164 * to[1]
1.00637 * t[1]
Active
Control
D
1.38211 * to[1]
1.02216 * t[1]
Active
Remission

Figure 2

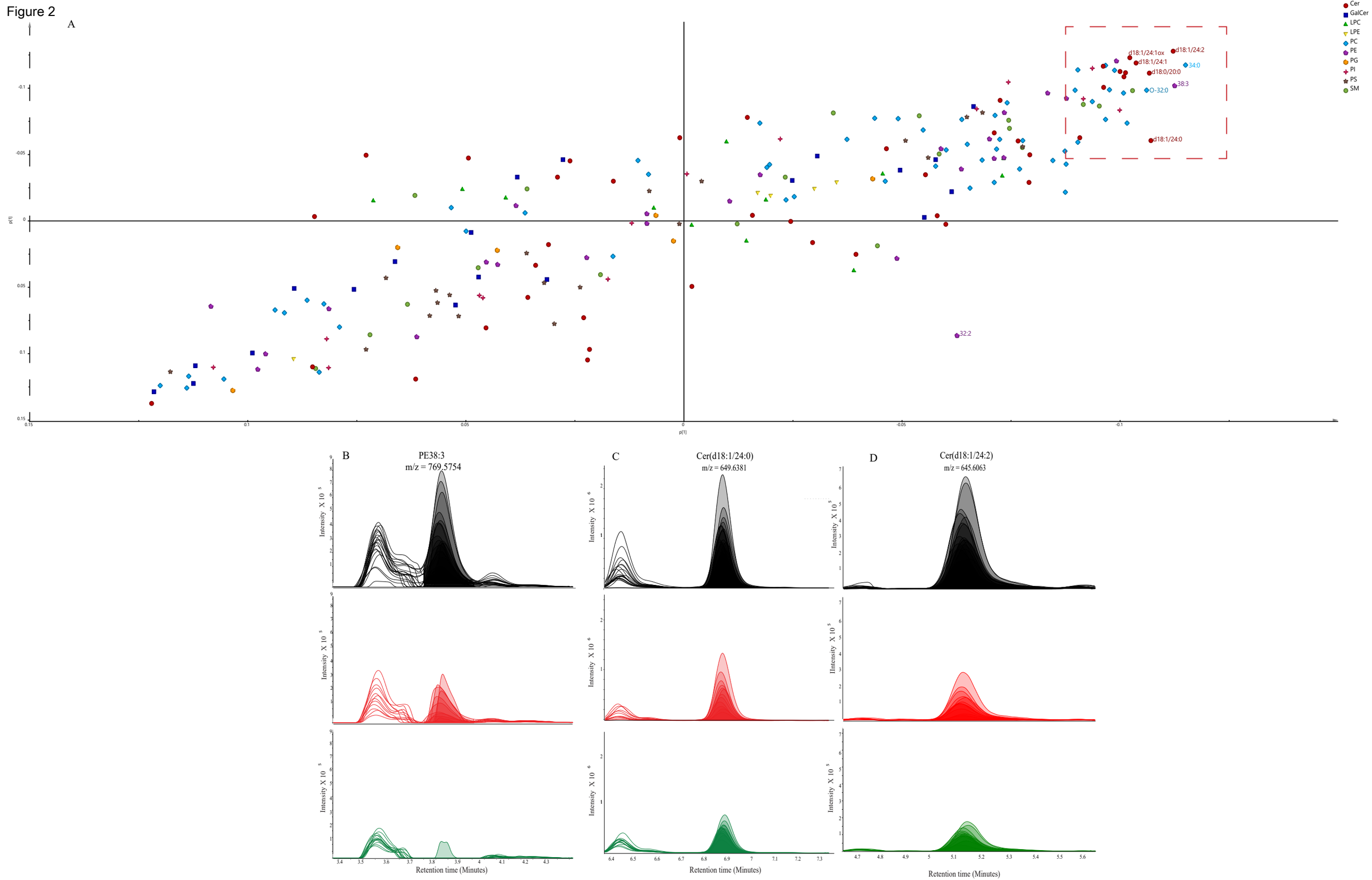
A
Cer
GalCer
LPC
LPE
PC
PE
PG
PI
PS
SM
d18:1/24:1ox
d18:1/24:2
d18:1/24:1
34:0
d18:0/20:0
38:3
O-32:0
d18:1/24:0
32:2
p[1]
B
PE38:3
m/z = 769.5754
C
Cer(d18:1/24:0)
m/z = 649.6381
D
Cer(d18:1/24:2)
m/z = 645.6063
Intensity X 10 5
Intensity X 10 6
Retention time (Minutes)

Supp. Table 1

Kruskal Wallis analysis comparing lipid species composition among the study groups

Lipids	Kruskal Wallis Test adj. p-value*	Active UC vs Healthy Control		Active UC vs Remission UC		Remission UC vs Healthy Control	
		Fold change	P.value**	Fold change	P.value**	Fold change	P.value**
Cer(d18:0/16:0)	0.160	0.91	0.702	0.79	0.018	1.16	0.067
Cer(d18:0/17:0)	0.099	0.83	0.063	0.74	0.016	1.12	0.565
Cer(d18:0/18:0)	<0.001	1.64	<0.001	1.60	<0.001	1.02	0.998
Cer(d18:0/19:0)	1.000	1.14	0.279	0.91	0.625	1.25	0.162
Cer(d18:0/20:0)	<0.001	1.86	<0.001	1.68	0.001	1.11	0.621
Cer(d18:0/22:0)	<0.001	1.85	<0.001	1.92	<0.001	0.96	0.739
Cer(d18:0/22:1)	0.079	1.31	0.025	1.34	0.024	0.98	0.912
Cer(d18:0/23:0)	0.012	0.83	0.045	1.36	0.095	0.61	0.001
Cer(d18:0/23:1)	0.457	1.41	0.118	0.77	0.643	1.84	0.072
Cer(d18:0/23:3)	0.452	1.45	0.075	1.29	0.161	1.12	0.784
Cer(d18:0/24:0)	0.012	0.94	0.357	1.65	0.009	0.57	0.001
Cer(d18:0/24:1)	0.011	1.00	0.349	1.58	0.009	0.63	0.001
Cer(d18:0/25:0)	<0.001	0.53	<0.001	1.05	0.842	0.50	<0.001
Cer(d18:0/25:1)	0.002	0.68	0.006	1.49	0.139	0.46	<0.001
Cer(d18:0/26:0)	0.008	0.77	0.005	1.28	0.419	0.61	0.001
Cer(d18:0/26:1)	0.000	0.64	<0.001	1.22	0.273	0.52	<0.001
Cer(d18:1/14:0)	0.000	0.56	0.002	0.38	<0.001	1.47	0.407
Cer(d18:1/15:1)ox	1.000	0.51	0.736	0.64	0.986	0.80	0.755
Cer(d18:1/16:0)	0.006	0.94	0.594	0.53	0.001	1.75	0.007
Cer(d18:1/16:1)	0.000	0.32	<0.001	0.38	<0.001	0.83	0.317
Cer(d18:1/17:0)	0.001	0.73	0.050	0.54	<0.001	1.34	0.061

Cer(d18:1/18:0)	0.330	1.04	0.643	0.80	0.086	1.29	0.047
Cer(d18:1/18:1)	0.096	0.83	0.037	0.60	0.024	1.39	0.803
Cer(d18:1/19:0)	0.111	1.21	0.022	0.96	0.833	1.26	0.028
Cer(d18:1/20:0)	0.001	1.50	<0.001	1.23	0.024	1.23	0.162
Cer(d18:1/20:1)	0.014	1.50	0.001	1.13	0.341	1.33	0.047
Cer(d18:1/20:3)	1.000	0.96	0.523	1.06	0.682	0.90	0.348
Cer(d18:1/20:5)	0.011	0.93	0.805	0.58	0.001	1.61	0.007
Cer(d18:1/22:0)	0.000	1.50	<0.001	1.05	0.338	1.42	0.002
Cer(d18:1/22:1)	0.000	2.31	<0.001	1.92	<0.001	1.20	0.332
Cer(d18:1/22:6)	0.772	0.80	0.159	0.82	0.185	0.98	0.988
Cer(d18:1/23:0)	1.000	1.07	0.212	1.00	0.998	1.07	0.275
Cer(d18:1/23:1)	<0.001	1.63	<0.001	1.47	0.001	1.11	0.326
Cer(d18:1/24:0)	<0.001	1.51	<0.001	1.15	0.052	1.31	0.006
Cer(d18:1/24:1)	<0.001	1.59	<0.001	1.33	0.003	1.19	0.106
Cer(d18:1/24:1)ox	<0.001	5.96	<0.001	4.28	<0.001	1.39	0.387
Cer(d18:1/24:2)	<0.001	2.31	<0.001	1.76	<0.001	1.31	0.141
Cer(d18:1/25:0)	1.000	1.04	0.672	1.08	0.319	0.96	0.586
Cer(d18:1/25:1)	0.070	1.18	0.011	1.15	0.058	1.03	0.623
Cer(d18:1/25:2)	0.036	1.31	0.005	1.03	0.946	1.27	0.018
Cer(d18:1/26:0)	0.074	1.24	0.011	0.99	0.967	1.25	0.029
Cer(d18:1/26:1)	0.002	1.31	<0.001	1.06	0.797	1.23	0.003
Cer(d18:1/26:2)	<0.001	2.22	<0.001	1.55	0.022	1.43	0.025
GalCer(d18:0/22:0)	0.013	0.59	0.001	0.90	0.484	0.66	0.027
GalCer(d18:1/14:0)	1.000	1.16	0.344	1.13	0.367	1.03	1.000
GalCer(d18:1/16:0)	0.001	0.66	0.001	0.45	0.001	1.48	0.858
GalCer(d18:1/18:0)ox	<0.001	0.50	<0.001	0.64	0.001	0.77	0.068
GalCer(d18:1/20:0)	0.047	1.57	0.015	0.91	0.604	1.72	0.009
GalCer(d18:1/20:3)	0.001	5.37	<0.001	2.10	0.348	2.55	0.007

GalCer(d18:1/22:0)	0.002	1.48	<0.001	1.00	0.979	1.47	0.002
GalCer(d18:1/22:0)ox	0.002	0.67	<0.001	0.87	0.297	0.78	0.015
GalCer(d18:1/22:1)	0.032	1.50	0.003	1.13	0.558	1.33	0.040
GalCer(d18:1/23:0)	1.000	0.89	0.384	0.83	0.226	1.07	0.726
GalCer(d18:1/24:0)	0.185	1.35	0.019	1.11	0.445	1.21	0.173
GalCer(d18:1/24:0)ox	0.000	0.55	<0.001	0.72	0.078	0.76	0.017
GalCer(d18:1/2:41)	0.000	2.66	<0.001	1.88	0.007	1.41	0.139
GalCer(d18:1/24:1)ox	0.068	0.90	0.129	1.18	0.123	0.77	0.006
GalCer(d18:1/25:0)ox	0.000	0.45	<0.001	0.64	0.012	0.70	0.020
GalCer(d18:1/25:1)ox	0.000	0.60	<0.001	0.75	0.016	0.80	0.033
GalCer(d18:1/26:0)ox	0.014	0.58	0.001	0.90	0.570	0.64	0.022
GalCer(d18:1/26:1)	0.179	0.73	0.021	0.94	0.737	0.77	0.088
GalCer(d18:1/26:1)ox	0.094	0.85	0.093	1.19	0.218	0.72	0.009
GalCer(d18:1/28:1)ox	0.825	0.90	0.110	0.88	0.635	1.02	0.334
LPC(14:0)	0.004	2.00	<0.001	1.13	0.361	1.77	0.019
LPC(16:0)	0.291	1.06	0.036	1.08	0.203	0.98	0.504
LPC(16:1)	0.007	1.65	0.001	1.13	0.983	1.46	0.005
LPC(17:0)	0.693	0.99	0.146	1.00	0.165	0.99	0.998
LPC(18:0)	1.000	0.98	0.684	0.98	0.260	1.00	0.498
LPC(18:1)	0.472	1.02	0.778	1.23	0.062	0.82	0.142
LPC(18:2)	0.002	1.71	<0.001	1.32	0.043	1.29	0.135
LPC(20:0)	0.365	1.17	0.912	0.83	0.064	1.41	0.072
LPC(20:5)	0.009	0.43	0.001	1.00	0.671	0.43	0.012
LPC(22:6)	0.246	0.65	0.044	1.04	0.893	0.63	0.059
LPC(O-16:1)	0.101	2.03	0.039	0.06	0.497	32.56	0.015
LPC(O-18:0)	0.140	0.50	0.016	1.00	0.689	0.50	0.081
LPE(16:0)	0.031	1.47	0.003	2.34	0.447	0.63	0.053
LPE(16:1)	0.345	7.99	0.061	6.58	0.121	1.21	0.828

LPE(18:0)	0.049	1.23	0.007	2.71	0.880	0.45	0.026
LPE(18:2)	1.000	2.90	0.533	3.35	0.613	0.86	0.311
LPE(20:0)	0.000	0.37	<0.001	0.40	<0.001	0.93	0.635
PC(30:1)	0.000	2.49	<0.001	1.58	0.029	1.58	0.078
PC(31:1)	0.001	1.49	<0.001	1.27	0.018	1.17	0.254
PC(32:0)	0.000	1.69	<0.001	1.34	0.008	1.26	0.010
PC(32:1)	0.009	1.27	0.001	1.03	0.476	1.24	0.023
PC(32:2)	0.008	1.71	0.001	1.25	0.130	1.37	0.105
PC(33:0)	0.000	1.90	<0.001	1.57	0.001	1.21	0.137
PC(33:1)	1.000	1.02	0.770	1.09	0.557	0.94	0.426
PC(33:2)	0.001	0.68	<0.001	0.74	0.003	0.93	0.638
PC(34:0)	0.000	1.93	<0.001	1.64	<0.001	1.18	0.541
PC(34:1)	0.000	0.83	<0.001	0.82	0.002	1.01	0.646
PC(34:2)	0.000	0.78	<0.001	0.80	<0.001	0.98	0.461
PC(34:3)	1.000	0.90	0.472	0.97	0.889	0.93	0.615
PC(34:4)	0.032	1.79	0.003	1.25	0.177	1.43	0.162
PC(35:0)	0.002	1.80	<0.001	1.52	0.010	1.18	0.418
PC(35:1)	0.094	0.84	0.029	1.12	0.604	0.75	0.017
PC(35:2)	0.004	0.70	<0.001	0.91	0.424	0.77	0.016
PC(35:3)	0.000	0.57	<0.001	0.67	0.006	0.84	0.163
PC(35:4)	0.001	2.50	<0.001	1.72	0.014	1.45	0.212
PC(36:1)	1.000	1.01	0.759	1.16	0.189	0.88	0.348
PC(36:2)	0.000	0.79	<0.001	0.84	<0.001	0.94	0.123
PC(36:3)	0.000	0.82	<0.001	0.91	0.241	0.90	0.002
PC(36:4)	0.004	1.26	<0.001	1.02	0.750	1.24	0.006
PC(36:5)	0.182	1.15	0.344	1.52	0.018	0.76	0.178
PC(36:6)	1.000	0.94	0.996	1.18	0.242	0.79	0.280
PC(37:2)	0.036	1.34	0.011	1.39	0.016	0.96	0.996

PC(38:3)	0.001	1.68	<0.001	1.55	0.005	1.09	0.486
PC(38:4)	0.001	1.54	<0.001	1.07	0.715	1.44	0.003
PC(38:5)	0.000	1.43	<0.001	1.22	0.040	1.17	0.058
PC(38:6)	0.020	1.45	0.003	1.33	0.027	1.09	0.578
PC(38:7)	0.874	1.16	0.354	1.30	0.127	0.89	0.554
PC(40:4)	0.000	2.59	<0.001	2.18	0.003	1.19	0.458
PC(40:5)	0.000	2.07	<0.001	1.49	0.057	1.39	0.057
PC(40:6)	0.016	1.49	0.001	1.16	0.185	1.28	0.105
PC(40:7)	0.152	1.00	0.900	1.20	0.021	0.83	0.045
PC(40:8)	0.019	1.35	0.067	1.79	0.002	0.75	0.209
PC(42:5)	0.000	2.58	<0.001	2.52	0.001	1.02	0.968
PC(O-32:0)	0.000	2.07	<0.001	1.68	0.001	1.23	0.303
PC(O-32:1)	0.015	1.50	0.003	1.43	0.016	1.05	0.716
PC(O-34:0)	1.000	1.10	0.556	1.16	0.207	0.95	0.519
PC(O-34:1)	0.202	1.22	0.208	1.49	0.022	0.82	0.318
PC(O-34:2)	0.001	0.59	<0.001	0.82	0.202	0.73	0.017
PC(O-34:3)	0.001	0.63	<0.001	0.86	0.196	0.73	0.019
PC(O-36:2)	0.010	0.72	0.013	1.24	0.250	0.58	0.001
PC(O-36:3)	0.000	0.37	<0.001	0.58	0.008	0.63	0.018
PC(O-36:4)	0.002	1.44	<0.001	1.22	0.060	1.18	0.119
PC(O-36:5)	0.013	1.27	0.001	1.05	0.581	1.21	0.020
PC(O-36:6)	0.778	0.77	0.105	0.91	0.386	0.85	0.532
PC(O-38:2)	1.000	1.35	0.239	1.26	0.472	1.08	0.711
PC(O-38:3)	0.000	1.68	0.010	2.05	<0.001	0.82	0.127
PC(O-38:4)	0.022	1.80	0.006	1.54	0.016	1.17	0.832
PC(O-38:5)	0.114	1.26	0.013	1.15	0.126	1.09	0.445
PC(O-38:6)	0.001	1.52	<0.001	1.42	0.003	1.07	0.659
PC(O-38:7)	0.264	1.35	0.028	1.18	0.330	1.15	0.302

PC(O-40:4)	0.000	3.80	<0.001	2.77	0.001	1.37	0.458
PC(O-40:6)	0.000	1.82	<0.001	1.59	0.001	1.14	0.553
PE(32:0)	0.028	1.53	0.003	1.13	0.630	1.35	0.030
PE(32:1)	0.183	1.43	0.069	0.77	0.481	1.86	0.025
PE(32:2)	0.003	1.45	0.076	0.72	0.017	2.02	<0.001
PE(34:0)	0.018	1.43	0.002	1.32	0.094	1.08	0.221
PE(34:1)	0.000	0.67	<0.001	0.79	0.010	0.86	0.107
PE(34:2)	0.107	0.82	0.053	0.80	0.020	1.03	0.665
PE(36:1)	0.174	0.92	0.036	1.07	0.794	0.86	0.038
PE(36:2)	0.564	0.87	0.112	0.96	0.820	0.91	0.109
PE(36:3)	1.000	0.93	0.988	1.00	0.509	0.93	0.553
PE(36:4)	0.002	1.54	<0.001	1.08	0.561	1.42	0.006
PE(36:5)	0.738	0.81	0.119	1.05	0.975	0.77	0.180
PE(38:0)	0.026	0.83	0.002	0.93	0.107	0.88	0.235
PE(38:2)	0.142	1.31	0.014	1.10	0.408	1.20	0.161
PE(38:3)	0.000	37.48	<0.001	1.96	0.009	19.13	0.020
PE(38:4)	0.002	1.46	<0.001	1.16	0.138	1.26	0.052
PE(38:5)	<0.001	2.17	<0.001	1.80	0.005	1.20	0.205
PE(38:6)	1.000	1.03	0.516	0.89	0.232	1.16	0.596
PE(40:4)	<0.001	2.66	<0.001	1.99	0.005	1.33	0.168
PE(40:6)	1.000	1.13	0.751	0.98	0.490	1.16	0.361
PE(40:7)	0.790	1.25	0.114	1.18	0.324	1.06	0.632
PE(42:5)	0.022	6.27	0.003	1.16	0.844	5.42	0.016
PE(O-34:2)	0.005	0.33	<0.001	0.48	0.036	0.69	0.258
PE(O-36:2)	<0.001	0.47	<0.001	0.84	0.364	0.56	0.001
PE(O-38:5)	<0.001	0.30	<0.001	0.45	0.001	0.65	0.185
PG(34:1)	0.341	0.92	0.038	1.04	0.557	0.89	0.201
PG(36:1)	0.633	1.08	0.472	0.90	0.225	1.19	0.080

PG(38:6)	0.000	0.32	<0.001	0.38	0.001	0.84	0.413
PG(40:7)	0.236	0.71	0.029	0.95	0.753	0.74	0.104
PG(40:8)	0.967	0.81	0.144	0.95	0.827	0.86	0.280
PG(45:8)	0.357	1.30	0.046	1.20	0.217	1.09	0.538
PI(34:0)	<0.001	2.25	<0.001	1.40	0.258	1.61	0.003
PI(34:1)	0.013	0.75	0.001	0.82	0.039	0.92	0.377
PI(34:2)	0.010	0.72	0.002	0.73	0.016	0.99	0.606
PI(35:2)	<0.001	0.94	0.001	0.95	<0.001	1.00	0.547
PI(36:2)	<0.001	0.56	<0.001	0.74	0.036	0.76	0.012
PI(36:3)	1.000	0.88	0.251	0.92	0.850	0.95	0.405
PI(38:2)	0.504	0.87	0.452	0.71	0.059	1.23	0.281
PI(38:3)	0.001	1.57	0.001	1.61	0.001	0.97	0.940
PI(38:4)	<0.001	1.23	<0.001	1.07	0.139	1.15	0.021
PI(38:5)	0.367	1.10	0.205	1.20	0.049	0.92	0.483
PI(38:6)	0.549	0.76	0.105	0.81	0.153	0.94	0.916
PI(40:4)	<0.001	1.97	<0.001	1.63	0.002	1.21	0.111
PI(40:5)	<0.001	1.59	<0.001	1.45	0.002	1.10	0.309
PI(40:6)	1.000	1.13	0.622	1.23	0.400	0.91	0.732
PS(32:1)	0.689	0.08	0.094	0.50	0.771	0.16	0.230
PS(34:0)	<0.001	0.58	<0.001	0.67	0.001	0.86	0.126
PS(34:1)	<0.001	0.46	<0.001	0.36	<0.001	1.25	0.769
PS(36:1)	0.008	0.70	0.002	0.72	0.012	0.98	0.680
PS(36:2)	0.101	0.85	0.080	0.74	0.014	1.15	0.473
PS(36:3)	0.079	0.88	0.275	0.67	0.007	1.32	0.128
PS(36:4)	1.000	0.88	0.342	0.82	0.190	1.07	0.711
PS(38:1)	0.515	1.33	0.073	1.17	0.229	1.14	0.641
PS(38:2)	0.012	0.77	0.005	0.72	0.007	1.07	0.967
PS(38:3)	0.032	1.45	0.017	1.50	0.009	0.97	0.766

PS(38:4)	0.049	0.72	0.025	0.51	0.012	1.40	0.739
PS(38:5)	0.001	5.14	<0.001	3.64	0.001	1.41	0.930
PS(39:7)	0.036	0.68	0.003	0.86	0.102	0.79	0.288
PS(40:0)	0.017	0.84	0.015	1.40	0.311	0.60	0.002
PS(40:2)	0.007	0.68	0.001	0.80	0.026	0.86	0.398
PS(40:3)	1.000	1.00	0.785	1.71	0.996	0.58	0.814
PS(40:4)	0.007	2.00	0.001	1.22	0.427	1.64	0.022
PS(40:5)	0.072	1.53	0.006	1.26	0.240	1.21	0.190
PS(40:6)	1.000	1.07	0.255	0.83	0.197	1.30	0.849
PS(40:7)	0.048	0.78	0.004	0.91	0.385	0.86	0.086
SM(d18:0/14:0)	0.006	1.39	0.006	1.50	0.002	0.93	0.640
SM(d18:0/16:0)	0.070	0.76	0.008	0.84	0.092	0.91	0.442
SM(d18:0/18:0)	1.000	1.03	0.622	0.97	0.609	1.06	0.367
SM(d18:1/14:0)	0.010	1.46	0.002	1.36	0.018	1.07	0.575
SM(d18:1/15:0)	0.105	1.24	0.045	1.29	0.023	0.96	0.739
SM(d18:1/16:0)	0.170	0.90	0.042	0.88	0.051	1.03	0.993
SM(d18:1/16:1)	<0.001	1.90	<0.001	1.61	0.004	1.18	0.345
SM(d18:1/18:0)	0.000	0.74	0.001	0.62	<0.001	1.19	0.256
SM(d18:1/18:0)ox	0.331	1.08	0.376	1.19	0.036	0.91	0.249
SM(d18:1/18:1)	0.019	0.81	0.016	0.64	0.004	1.26	0.602
SM(d18:1/19:0)	0.022	1.08	0.286	1.42	0.002	0.76	0.051
SM(d18:1/20:0)	1.000	0.92	0.526	0.90	0.593	1.02	0.949
SM(d18:1/21:1)	0.004	0.75	0.006	1.25	0.233	0.60	<0.001
SM(d18:1/22:0)	0.926	1.17	0.237	0.94	0.652	1.24	0.146
SM(d18:1/23:2)	0.000	1.88	<0.001	1.79	<0.001	1.05	0.984
SM(d18:1/24:0)	0.015	1.33	0.192	1.68	0.001	0.79	0.065
SM(d18:1/24:1)	0.003	1.44	<0.001	1.29	0.018	1.12	0.351
SM(d18:1/24:2)	<0.001	1.66	<0.001	1.40	0.004	1.18	0.207

SM(d18:1/25:1)	0.008	0.75	0.005	1.17	0.466	0.64	0.002

* Kruskall Wallis p values adjusted by Benjamini-Hocheberg method
** Dunn post hoc test p values

Supp. Figure 1